

On the Crucial Role of Wind-Wave-Tunnel Studies to Reveal the Mechanisms of Air-Sea Gas Exchange

Bernd Jähne^{1,2}

¹Interdisziplinäres Zentrum für Wissenschaftliches Rechnen (IWR)
and ²Institut für Umweltphysik, Heidelberg University
Bernd.Jaehne@iwr.uni-heidelberg.de

Session OS1.7 Impacts of Air-Sea Fluxes on Biogeochemistry and Climate: Challenges and Opportunities
from 20 years of Surface Ocean Lower Atmosphere Study (SOLAS)

ITS2.7/AS2.7, EGU General Assembly, 15 April 2024



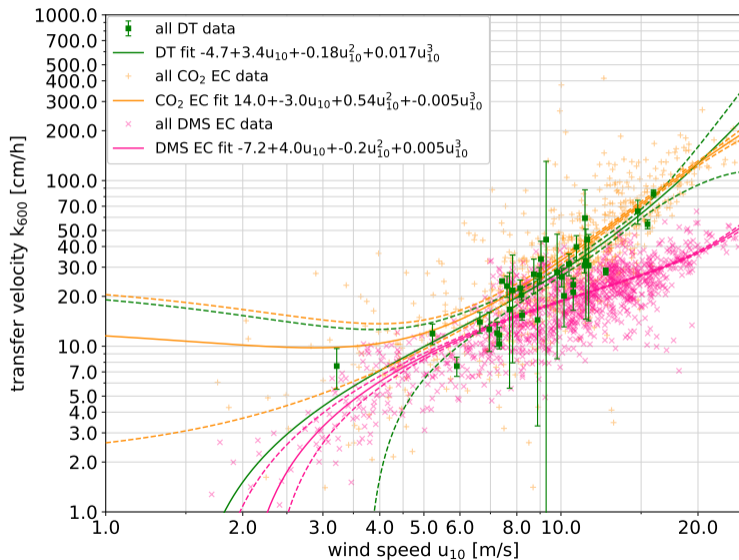
Major challenge since half a century

Large uncertainty in gas transfer velocity and the parameters controlling it

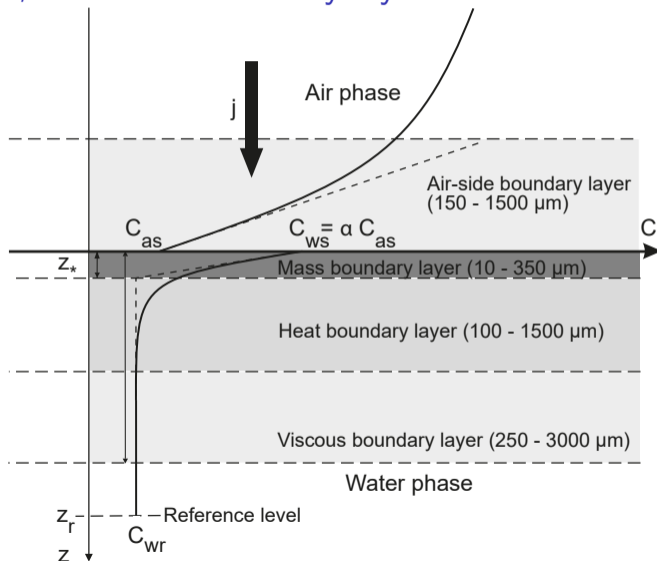
- Wind is major driving factor, but
- Energy input split into generating shear current and wind-wave field
- \rightsquigarrow **Turbulence** generation by **shear flow** and **breaking waves**
- **Bubbles** submerged by breaking waves generate additional exchange surface
- All these processes are influenced by **surfactants** at water surface



Recent collection of field data



Viscous, thermal, and mass boundary layers on both sides



Basic scales for exchange across air-water interface I

- Speed of exchange: **transfer velocity** k [cm/h]

$$k = \frac{j}{\Delta C} = \frac{j}{c_{ws} - c_{wr}} \quad (2 - 70 \text{ cm/h}) \quad (1)$$

- Vertical spatial scale: **mass boundary layer thickness** z_* [μm]

$$j = -D \left. \frac{\partial c}{\partial z} \right|_0 = -D \frac{\Delta c}{z_*} \quad \rightsquigarrow \quad z_* = \frac{D}{k} \quad (350 - 10 \mu\text{m}) \quad (2)$$

Basic scales for exchange across air-water interface II

- Temporal scale **time constant** t_\star [s]

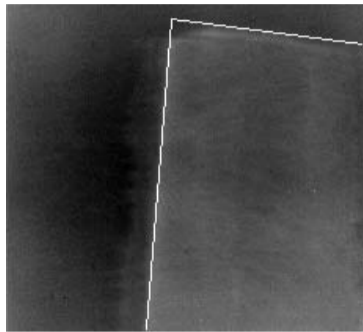
$$t_\star = \frac{z_\star}{k} = \frac{D}{k^2} \quad (60 - 0.06 \text{ s}) \quad (3)$$

- Horizontal spatial scale **time constant** x_\star [m] (footprint required)

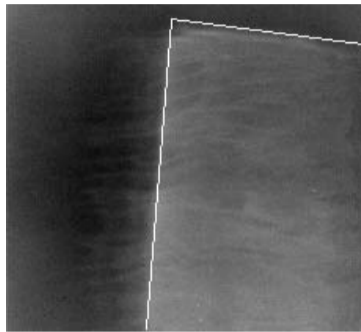
$$x_\star = \Delta u t_\star \quad (100 - 1 \text{ cm}) \quad (4)$$

Relevant is not advection but velocity difference Δu caused by the shear current within the viscous boundary layer

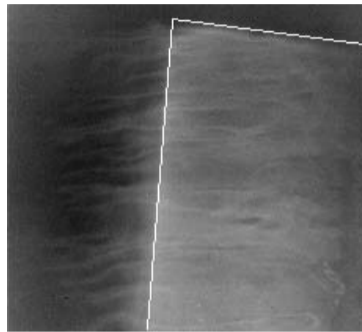
Active thermography: Spatiotemporal response at 2.0 m/s wind speed



0.5 s



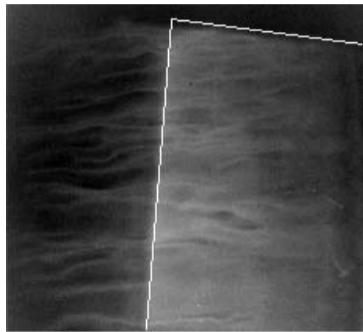
1.0 s



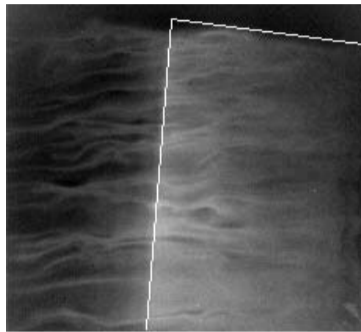
1.5 s

Time after switching on heat flux with CO₂ laser in marked areas
image sector 25 cm × 25 cm

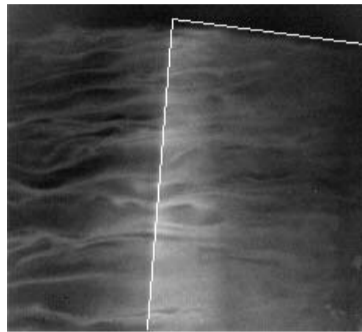
Active thermography: Spatiotemporal response at 2.0 m/s wind speed



2.0 s



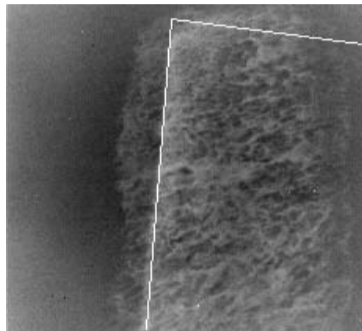
2.5 s



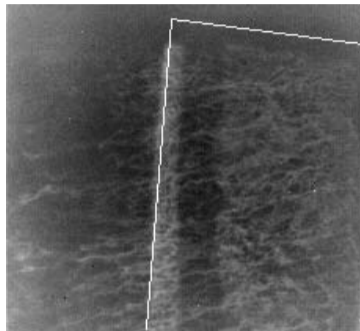
3.0 s

Time after switching on heat flux with CO₂ laser in marked areas
image sector 25 cm × 25 cm

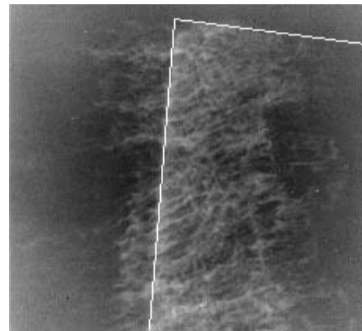
Same at medium wind speed (7.0 m/s)



0.5 s



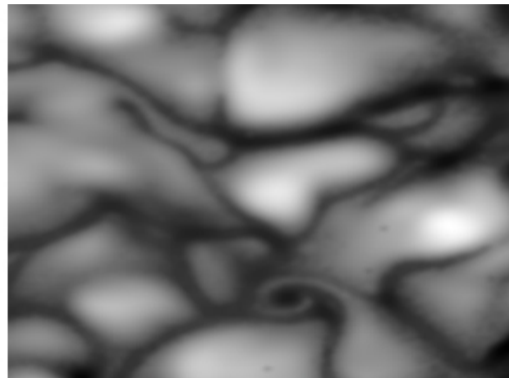
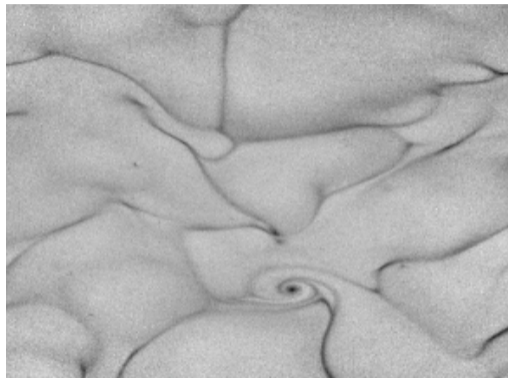
1.0 s



1.5 s

Time after switching on heat flux with CO₂ laser in marked areas
image sector 25 cm × 25 cm

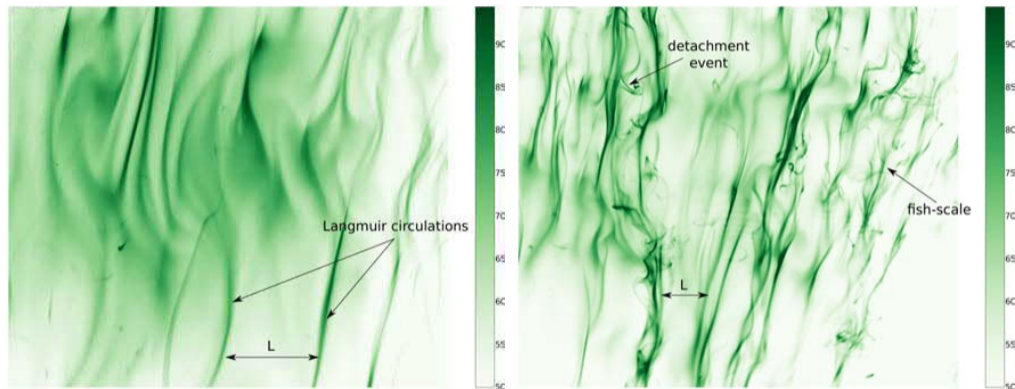
Imaging of concentration fields within mass boundary layer



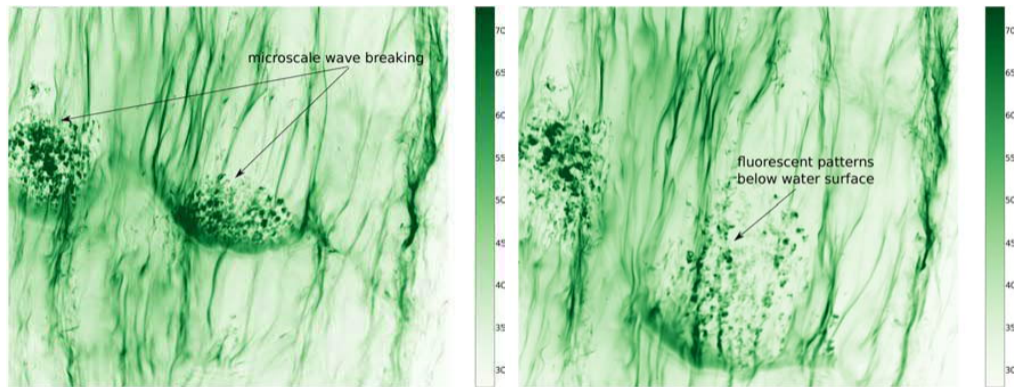
No wind, convection induced (left oxygen, right heat)
(from Kunz, Bachelor thesis, 2011)



Imaging of concentration fields within mass boundary layer



Imaging of concentration fields within mass boundary layer



3.88 m/s (*Trofimova, PhD 2015, Heidelberg University*)



Large Heidelberg Annular Air-Sea Interaction Facility (Aeolotron)

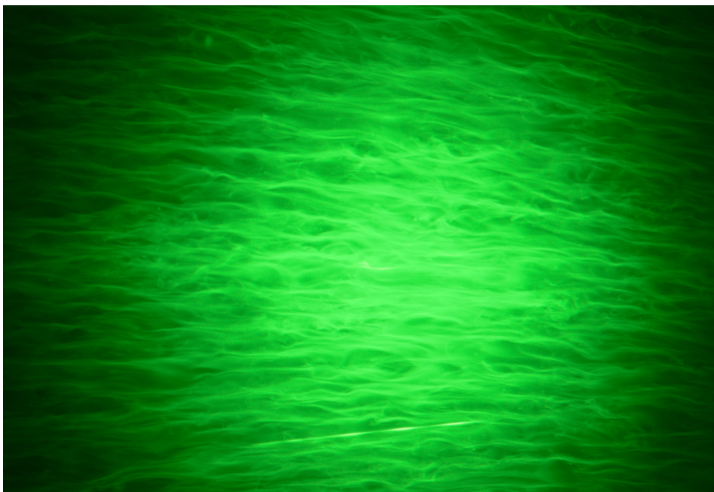


Outlook with Preliminary Results At Low and Very High Wind Speeds

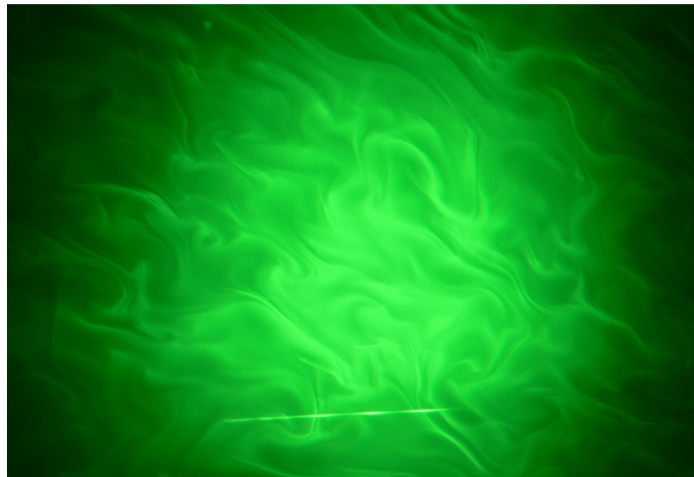
- Insoluble hexadecanol monolayer and 5 ppm Triton X-100 completely suppress wind-wave generation up to 8 m/s wind speed
- In contrast, 2.4 g/L hexanol reducing surface tension to 43 dyn/cm does not suppress wind-waves at all
- No visible difference in spatio-temporal structures of concentration fields with monolayer of hexanol and 5 ppm Triton X-100



5 ppm Triton X-100 at ≈ 4 m/s Wind Speed



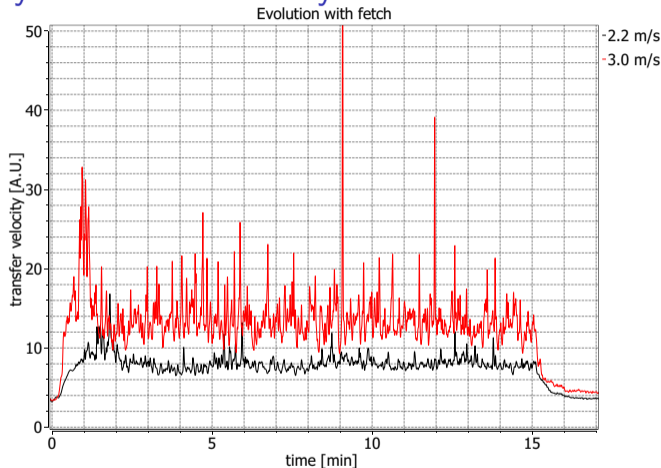
Switching Wind Off



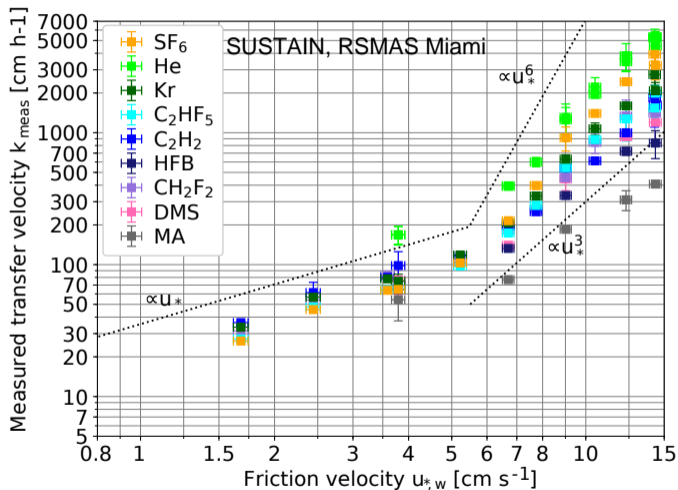
Seconds after wind is turned off, patterns change, gas transfers dies away



Fetch dependency of transfer velocity



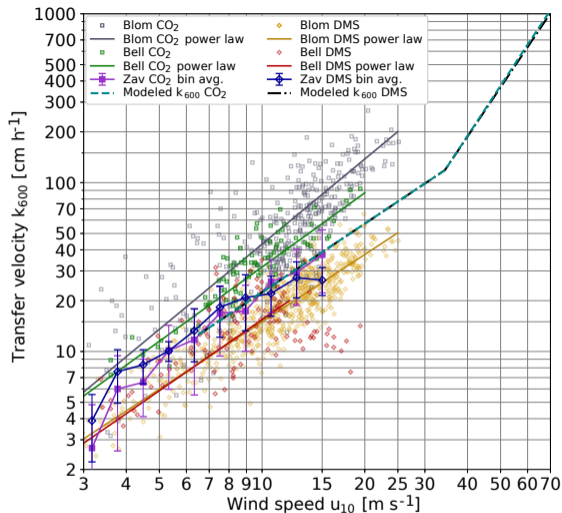
Very High Wind Speeds: New Regime beyond 35 m/s



(Krall et al., 2019)



Very High Wind Speeds DMS and CO₂



No significant difference between $k(\text{CO}_2)$ and $k(\text{DMS})$ scaled to $Sc = 600$
according to results from Kyoto and SUSTAIN facilities



Conclusions

- Novel imaging techniques directly reveal mechanisms of air-sea gas transfer
- Large annular facility provides sufficiently realistic oceanic conditions
- A physically-based model will emerge from the novel approach within two years including the effects of sea state, unsteady winds and surfactants



Extra Material



Modeling Bubble-induced Gas Transfer I

- Bubbles provide additional closed exchange surface

$$k_{\text{tot}} = k_s + k_c \quad (5)$$

- Limiting case of low solubility: like open surface

$$k_{c,\text{low}\alpha} = k_{c,600} \left(\frac{600}{Sc} \right)^{n_b} \quad (6)$$

- Limiting case of high solubility: bubble carries gas with volume flux Q_b

$$k_{c,\text{high}\alpha} = \frac{1}{\alpha} \frac{Q_b}{A_s} = \frac{k_r}{\alpha} \quad (7)$$

Transfer velocity $\propto k_r = Q_b/A_s$ and to $1/\alpha$; does not depend on Schmidt number

Modeling Bubble-induced Gas Transfer II

- Exponential transition between the two limiting cases

$$k_c = \frac{k_r}{\alpha} \left[1 - \exp\left(-\frac{\alpha}{\alpha_t}\right) \right] \quad \text{with} \quad \alpha_t = \frac{k_r}{k_{c,600}} \left(\frac{Sc}{600} \right)^{n_b} \quad (8)$$

- Limiting k_{tot} for clean water ($n = n_b = 0.5$)

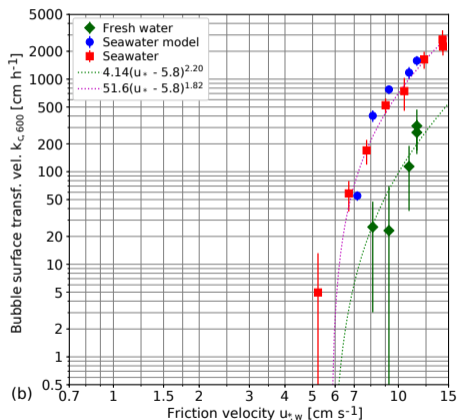
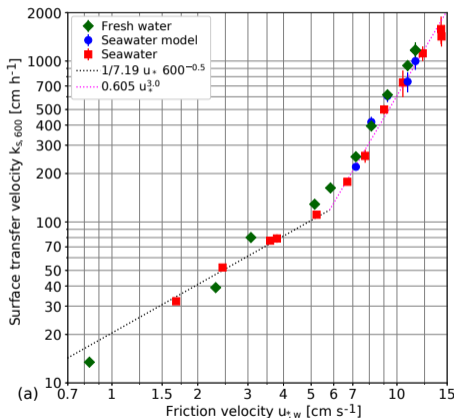
$$k_{\text{tot}} = \begin{cases} (k_{s,600} + k_{s,600}) \left(\frac{600}{Sc} \right)^{0.5} & \alpha \ll \alpha_t \\ k_{s,600} \left(\frac{600}{Sc} \right)^{0.5} + \frac{k_r}{\alpha} & \alpha \gg \alpha_t \end{cases} \quad (9)$$

Just two parameters for bubble-induced gas exchange: $k_{c,600}$ and k_r



Verification of Model with Multi-Tracer Measurements

from two high wind speed facilities: Kyoto and SUSTAIN (*Krall et al., 2019*)



Verification of Model with Multi-Tracer Measurements

from two high wind speed facilities: Kyoto and SUSTAIN (*Krall et al., 2019*)

